Wen and Yanovski, J Obes Weight Loss Ther 2013, 3:6
DOI: 10.4172/2165-7904.1000202

Journal of
Obesity & Weight Loss Therapy

Research Article Open Access

A Phenomenon found in the Transcriptional Regulation Study on Mouse Melanocortin 3 Receptor—Link the Transcriptional Activity with the Phosphorylation and Glycosylation of Transcription Factors

Xin Wen[1]* and Jack A Yanovski[2]
[1]*Developmental Neurobiology Section, NHLBI, NIH, USA*
[2]*UGO, Eunice Kennedy Shriver, NICHD, NIH, USA*

Abstract

Melanocortin 3 receptor (MC3R) is involved in the regulation of energy homeostasis. Study on mouse MC3R promoter has been performed following the determination of its transcription starting site, mouse MC3r deletion constructs were built by sub cloning into pGL3 vector, then the gene reporter assay of the seven deletion constructs was tested by Dual Luciferase Assay.

On the other hand, phosphorylation and glycosylation play an important role in the transcription regulation. The global distribution of phosphorylation and glycosylation on transcription factor could be found in open source database.

In this report, relative luciferase activity and the distribution of phosphorylation-glycosylation sites on promoter model transcription factor were plotted, for the first time, on the same chart, within a 3.2 kb upstream the methinoin ATG, the two trend lines of the relative luciferase activity and the distribution of phophorylation-glycosylation sites, they were found tend to be negative reciprocal.

Keywords: Transcirptional regulation; Promoter; Epigenetic control; 5'UTR; Promoter model

Abbreviations: MC3R: Melanocortin 3 Receptor; MC3r: Melanocortin 3 Receptor Genes; 5'UTR: 5 Untranslated Region; DLA: Dual Luciferase Assay

Introduction

Melanocortin 3 receptor (MC3R) is expressed at high levels [1-3], in the arcuate nucleus and ventromedial nucleus, and mainly controls the conversion of food to fat, nutrient partitioning and build-up of lean mass. It is also shown that the MC3R may affect body fat [4] and food intake through both central and peripheral mechanisms. Simultaneously, of the five known members of signal peptide related rhodopsin GPCRs, promoter study of other melanocortin receptors promoters (MC1r [5], MC4r [6], and MC5r [7]) stimulates the study of MC3R promoter.

Furthermore, primary gene induction or repression in eukaryotes does not require protein synthesis, suggesting the involvement of posttranslational modifications [8]. Since many different types of stimuli that affect gene expression also lead to the activation of protein kinases, analysis of transcription factor phosphorylation is essential for complete understanding of the signal pathways. The activity of transcription factors maybe modulated by their signal-sensing domain including phosphorylation [9]. In addition, a nutrient sensitive sugar modification, glycosylation interface with the epigenetic control of gene expression.

The curiosity to the regulatory complex, the activity of transcription machinery, the range of regulatory mechanism and the post translation modification in the epigenetic transcription regulation made us start the promoter study of MC3R.

Materials and Methods

Determination of transcription starting site of mMC3r using 5'RACE

Determination of transcription starting site by 5'RACE was performed on total *Mus musculus* hypothalamus total RNA using the 5'RLM-RACE kit (Ambion, Invitrogen). Total mouse hypothalamus RNA treated [10] with CIP (Calf Intestine Alkaline Phosphatase) to remove free 5'-phosphates then treated with TAP (Tobacco Acid Pyrophosphatase) to remove the cap structure from full-length mRNA (exposing a 5'-monophosphate). A RNA adapter oligonucleotide was then ligated to the full-length RNA species using T4 RNA ligase. First-strand cDNA was synthesized twice, using random decamers and gene-specific RT primers. We amplified 5' cDNA ends using a nested PCR approach, where the nested 5' primers were specified by the adapter oligonucleotide sequence and the nested 3' primers were MC3R-specific. PCR products were then sub-cloned for sequencing.

Cloning of 5' flanking mMC3r luciferase reporter vectors

Serious deletion fragments was constructed using 7 forward primers ranging from 3174 bp to 373 bp respectively, and reverse primer 116 bp upstream ATG (Table 1), by PCR amplification with template of 3.2 kb 5'flanking from *Mus musculus* (C57BL/6J) assembly sequence. Series deletion fragment containing sequences extending from 3084 bp to 283 bp were subcloned into the upstream of the firefly luciferase gene in pGL3 vector.

Cell transfection and Dual Luciferase Assays (DLA)

Human HEK293 was transiently transfected using FuGENE'6 Transfection Reagent (Roche). 48 hours after transfection and over 65% cell confluency, add luciferase reagent and measure at luminometer OPTIMA (BMG LABTECH). Renilla was cotransfected and used to

***Corresponding author:** Xin Wen, Developmental Neurobiology Section, NHLBI, NIH, USA, Tel: +1 301 496 2651; Fax: +1 301 402 0574; E-mail: xin.wen@nih.gov

Received November 26, 2013; **Accepted** December 17, 2013; **Published** December 19, 2013

Citation: Wen X, Yanovski JA (2013) A Phenomenon found in the Transcriptional Regulation Study on Mouse Melanocortin 3 Receptor—Link the Transcriptional Activity with the Phosphorylation and Glycosylation of Transcription Factors. J Obes Weight Loss Ther 3: 202.doi:10.4172/2165-7904.1000202

Name of Primer	Sequence	From (bp)	To (bp)	P length (bp)
P1 forward	GACAGCTTGTGGATCTGTTTACAAACA	-3174	-3148	-3084
P2 forward	AGGGTCTGCAAAGTATAGCTCCCATCT	-2170	-2144	-2080
P3 forward	TCTGTCACATCCCAACTTGACACAAA	-1178	-1153	-1088
P4 forward	AAGGGCCAGGAGCAGTTGACATACTT	-978	-953	-888
P5 forward	GTCAATGTGTGAGCACAATTCTCTGA	-765	-740	-675
P6 forward	AGCAGCAGAATGAATGCTGATCTCTCT	-604	-578	-514
P7 forward	TTCTCACATCTAGCGTCAAGTCCCA	-373	-349	-283
reverse	ACTAAAGTCTAGACTGGACAGCATCCA	-116	-90	-26

Primer design was done by Dr. Ethan Sanford previously.

Table 1: Primer design for mMC3r deletion constructs.

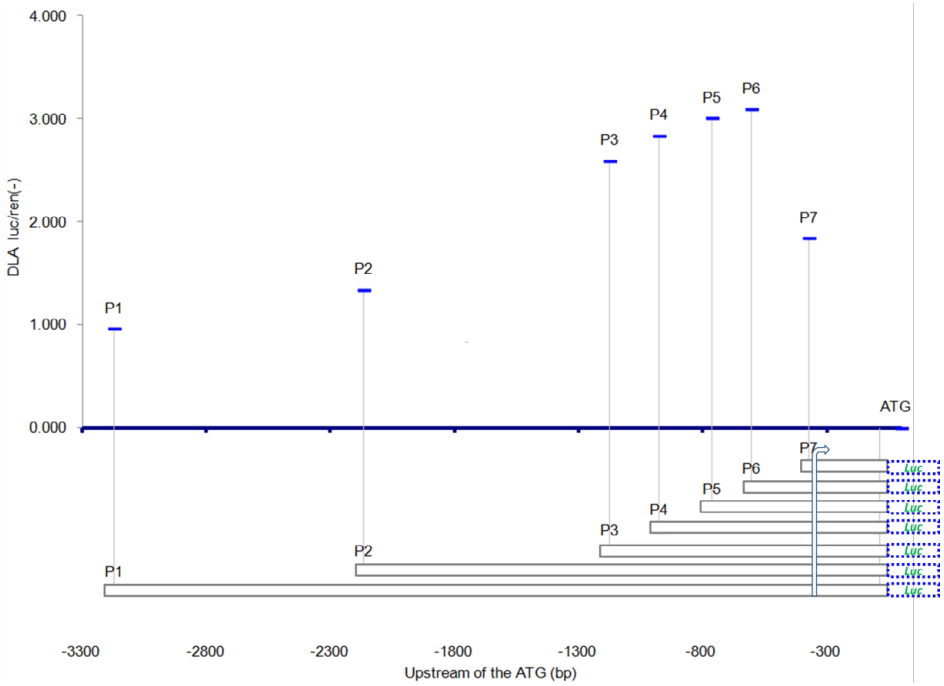

Figure 1a: Schematic structure of the luciferase reporter constructs (P1-P7) and DLA.

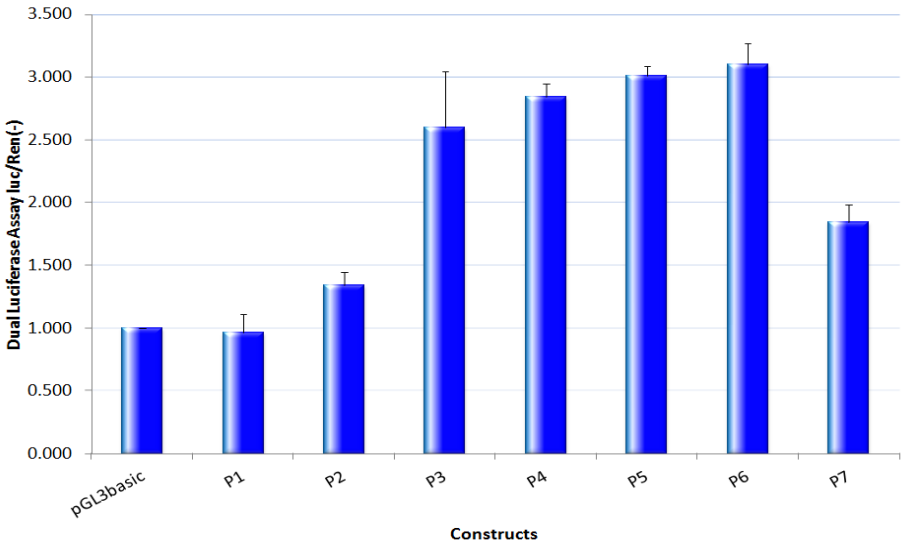

Figure 1b: Dual Luciferase Assay of mMC3r constructs plasmid P1-P7.

normalize the transfection efficiency. Assay was tested by triplicates on independent experiments.

Glycosylation and phosphorylation sites of promoter models

Promoter model [11] [A promoter model represents a framework of two or more conserved elements (e.g., transcription factor binding sites) with a defined distance (and strand orientation). Usually, promoter models are much more specific than single elements like transcription factor binding sites. Therefore, a promoter model can give higher evidence that the matching sites are functional.] Of the corresponding deletion constructs were inspecting by Genomatix, the glycosylation or phosphorylation sites on the model element (transcription factors) of promoter model were searched by Protein Knowledgebase of Uniprot.

Results and Discussion

Determination of the transcriptional start sites of the *Mus musculus* MC3r by 5'RLM RACE

Sequence analysis of the amplified products obtained by 5'RLM RACE performed on mouse hypothalamic RNA mapped [12] four initiations of transcription sites. Of those, a major site, at position -368bp from the initiating methionine, is corresponding to the predicted transcription start site according to GenBank. Additional sites were found at -432bp, -351bp and -347bp from the translational start site ATG.

Gene reporter assay in study of transcriptional activation and regulation of mMC3r

The reporter vectors of 7 kinds of mMC3r promoter deletion mutants were successfully constructed (Figure 1a), as confirmed by restriction enzyme digestion and sequencing. The activities of all constructs in pGL3 basic in HEK293 are shown (Figure 1b). The relative luciferase activity won't be changed a lot from P3 to P4 (2.596 to 2.844), P5 and P6 (3.010 to 3.098), and there is an obvious decrease from P6 (3.098) to P7 (1.845), at the same time, a significant increase was found from P2 (1.343) to P3 (2.596). Therefore, there should be core promoter sequences that are chopped between the -604bp (Table 1) to -373bp, there must be transcription repressor between the 2170 bp to 1178 upstream of the methionine ATG.

Promoter activity in response to forskolin or PMA stimuli

Forskolin, the potent activator of adenylate cyclase system and the biosynthesis of cyclic AMP, stimulated gene transcription by phosphorylation of CREB at serine 133 [13] and PMA (phorbol-12-myristate-13-acetate) potentiated the effect of low forskolin concentractions on CRH transcription and CREB phosphorylation [14]. Investigation whether the promoter activity is induced in response to forskolin or PMA stimuli has been performed. As it shown in Figure 2, Forskolin stimulate Dual Luciferase Activity in constructs P5 and P6. While PMA suppress a little bit compare with that of none treated (basal) expression.

Glycosylation and phosphorylation sites inspect and search on mMC3r promoter models

It should be noted: not *O*-GlcNAcylation but glycosylation could be found in database. As it shown in Table 3, On P1 , start from -3114 bp , there are G site on model E2FF_SP1F_01 at -3054 bp , from TF V$SP1F ; G site on model CEBP_CREB_01 at -2812 bp , from TF V$CREB ; G site on model NFKB_SP1F_04 at -2438 bp , from TF V$SP1F ; G site on model EGRF_SP1F_01 at -2383 bp , from TF V$SP1F ; G site on model KLFS_SP1F_01 at -2383 bp , from TF V$SP1F ; G site on model NR2F_SF1F_01 at -2278 bp , from TF V$SP1F . On P2 , start from -2170 bp , there are G site on model SMAD_EBOX_02 at -1982 bp , from TF V$EBOX ; G site on model CEBP_EBOX_01 at -1982 bp , from TF V$EBOX ; G site on model CREB_EBOX_02 at -1982 bp , from TF V$CREB ; G site on model CREB_EBOX_02 at -1982 bp , from TF V$EBOX ; G site on model EBOX_SREB_01 at -1982 bp , from TF V$EBOX ; G site on model EBOX_SREB_01 at -1982

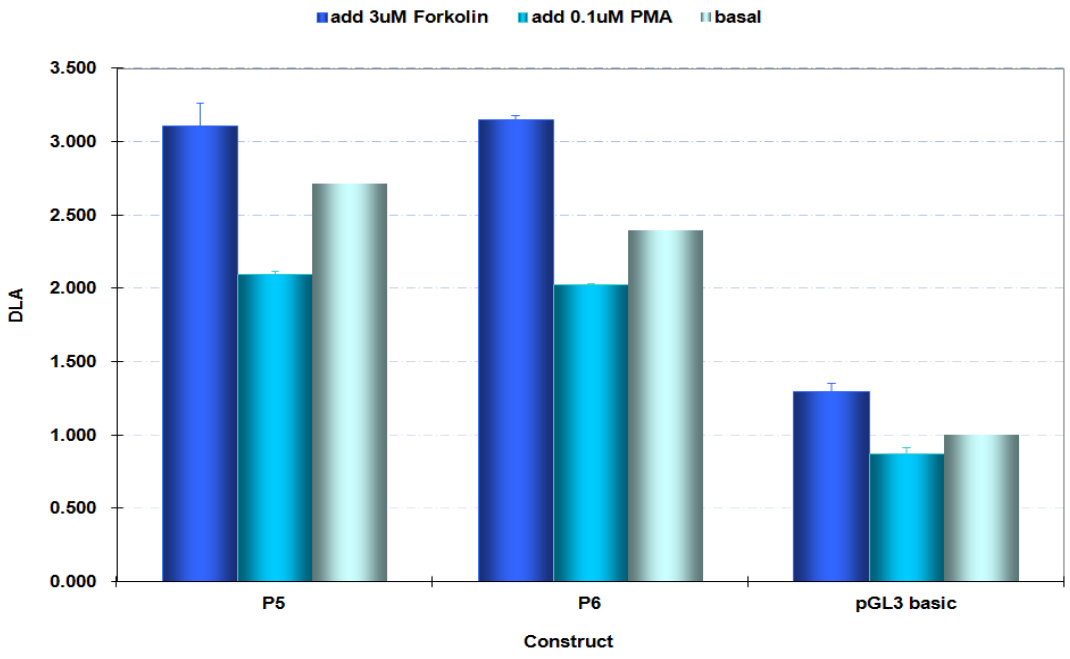

Figure 2: Treatment with stimulies Foskolin and PMA.

	Trend line Equation	R^2
DLA	y = -8E-14x5 - 3E-10x4 - 4E-07x3 - 0.0003x2 - 0.071x - 4.1812	0.9982
[G]	y = 6E-13x5 + 2E-09x4 + 2E-06x3 + 0.0012x2 + 0.223x + 13.725	0.9973
[P]	y = 2E-12x5 + 6E-09x4 + 7E-06x3 + 0.0038x2 + 0.7539x + 58.015	0.9998
[P]-[G]	y = 1E-12x5 + 4E-09x4 + 5E-06x3 + 0.0027x2 + 0.5309x + 44.29	1
[P]+[G]	y = 2E-12x5 + 8E-09x4 + 1E-05x3 + 0.005x2 + 0.977x + 71.74	0.9995

Table 2: Trend line equation and R square value.

Promoter Model	Sequence	bp	PTM	TF
P1		-3114		
E2FF_SP1F_01	GCTCAGGGTGGGTTTGG	-3054	G	V$SP1F
CEBP_CREB_01	CCCAGCTGAGGAAATTATTTT	-2812	G	V$CREB
NFKB_SP1F_04	GCCCTGGGCAGAGGCCC	-2438	G	V$SP1F
EGRF_SP1F_01	GATGTGGGCGGGACCAA	-2383	G	V$SP1F
KLFS_SP1F_01	GATGTGGGCGGGACCAA	-2383	G	V$SP1F
NR2F_SF1F_01	TTGCCAAGGACCCGT	-2278	G	V$SP1F
P2		-2170		
SMAD_EBOX_02	TAGACACGTGCTC	-1982	G	V$EBOX
CEBP_EBOX_01	TAGACACGTGCTC	-1982	G	V$EBOX
CREB_EBOX_02	GGTAGAGCACGTGTCTAATAA	-1982	G	V$CREB
CREB_EBOX_02	TAGACACGTGCTC	-1982	G	V$EBOX
EBOX_SREB_01	TAGACACGTGCTC	-1982	G	V$EBOX
EBOX_SREB_01	TAGACACGTGCTC	-1982	G	V$EBOX
EBOX_SREB_01	AGAGCACGTGTCT	-1981	G	V$EBOX
EBOX_SREB_01	AGAGCACGTGTCT	-1981	G	V$EBOX
P3		-1178		
P4		-978		
SORY_ETSF_01	CATTGACAATATTGCAGCTGTCACC	-773	G	V$SORY
P5		-765		
SP1F_YY1F_01	GGCGGTGGCGGGGGTCG	-704	G	V$SP1F
ETSF_SP1F_05	GGCGGTGGCGGGGGTCG	-704	G	V$SP1F
E2FF_SP1F_01	GGGAAGGGCTGGGCCAG	-686	G	V$SP1F
SP1F_ETSF_01	GGGAAGGGCTGGGCCAG	-686	G	V$SP1F
P6		-604		
SP1F_ETSF_04	GCAGGGGGCGCCAATCT	-517	G	V$SP1F
SP1F_MYOD_01	GCAGGGGGCGCCAATCT	-517	G	V$SP1F
P7		-373		

Table 3: Glycosylation site on promoter model of mMC3r.

bp , from TF V$EBOX[from different promoter module (promoter modules form a functional unit, allowing synergistic or antagonistic effects for a specific activation or repression of a gene) of the same promoter model] ; G site on model EBOX_SREB_01 at -1981 bp , from TF V$EBOX ; G site on model EBOX_SREB_01 at -1981 bp , from TF V$EBOX . On P4, start from -978 bp , there are G site on model SORY_ETSF_01 at -773 bp , from TF V$SORY . On P5 , start from -765 bp , there are G site on model SP1F_YY1F_01 at -704 bp , from TF V$SP1F ; G site on model ETSF_SP1F_05 at -704 bp , from TF V$SP1F ; G site on model E2FF_SP1F_01 at -686 bp , from TF V$SP1F ; G site on model SP1F_ETSF_01 at -686 bp , from TF V$SP1F. on P6, start from -604 bp, there are G site on model SP1F_ETSF_04 at -517 bp , from TF V$SP1F ; G site on model SP1F_MYOD_01 at -517 bp , from TF V$SP1F .

As it shown in Table 4, between P1 and P2, there are phosphorylation site on promoter model: there are P site Phosphorylation site) on model E2FF_SP1F_01 at -3054 bp, from TF V$SP1F ; P site on model E2FF_SP1F_01 at -3036 bp, from TF V$E2FF ; P site on model ETSF_ETSF_02 at -2897 bp, from TF V$ETSF ; P site on model IRFF_ETSF_02 at -2897 bp, from TF V$ETSF ; P site on model IRFF_ETSF_02 at -2892 bp, from TF V$IRFF ; P site on model ETSF_ETSF_02 at -2884 bp, from TF V$ETSF ; P site on model EGRF_NFAT_01 at -2815 bp, from TF V$NFAT ; P site on model CEBP_CREB_01 at -2812 bp, from TF V$CREB ; P site on model CEBP_CREB_01 at -2811 bp, from TF V$CEBP ; P site on model HAND_GATA_02 at -2806 bp, from TF V$HAND ; P site on model HAND_GATA_02 at -2789 bp, from TF V$GATA ; P site on model GATA_MYOD_01 at -2741 bp, from TF V$MYOD ; P site on model GATA_MYOD_01 at -2683 bp, from TF V$GATA ; P site on model SMAD_AP1F_03 at -2651 bp, from TF V$AP1F ; P site on model OCT1_CEBP_01 at -2593 bp, from TF V$OCT1 ; P site on model OCT1_CEBP_01 at -2583 bp, from TF V$CEBP ; P site on model NFKB_SP1F_04 at -2472 bp, from TF V$NFKB ; P site on model SMAD_EBOX_02 at -2462 bp, from TF V$SMAD ; P site on model SMAD_AP1F_03 at -2462 bp, from TF V$SMAD ; P site on model NFKB_SP1F_04 at -2438 bp, from TF V$SP1F ; P site on model EGRF_SP1F_01 at -2383 bp, from TF V$SP1F ; P site on model KLFS_SP1F_01 at -2383 bp, from TF V$SP1F ; P site on model KLFS_SP1F_01 at -2367 bp, from TF V$KLFS ; P site on model NR2F_SF1F_01 at -2278 bp, from TF V$SP1F ; P site on

Promoter Model	Sequence	bp	PTM	TF	Promoter Model	Sequence	bp	PTM	TF
PBXC_MYOD_01	GCAGAGGCTGACAGCTT	-3177	P	V$PBXC	SORY_SF1F_01	TGCCTGCAATCCCTGCAGTCGGCAC	-1317	P	V$SORY
PBXC_MYOD_01	GGCTGACAGCTTGTGGA	-3172	P	V$MYOD	NF1F_NR2F_01	CATAGTGAGTTCAAAGCCAGCCTGG	-1250	P	V$NR2F
P1		-3114			NF1F_NR2F_01	GGGTATCACCTATGCCAGGCT	-1234	P	V$NF1F
E2FF_SP1F_01	GCTCAGGGTGGGTTTGG	-3054	P	V$SP1F	P3		-1178		
E2FF_SP1F_01	GGGAGGCGGGGATCTGC	-3036	P	V$E2FF	CAAT_AP1F_01	CCCTGACCAATCA	-1049	P	V$AP1F
ETSF_ETSF_02	CTGTGAGGGGAAGTTGAGATC	-2897	P	V$ETSF	CAAT_CAAT_01	CTGACCAATCAAGAG	-1046	P	V$CAAT
IRFF_ETSF_02	CTGTGAGGGGAAGTTGAGATC	-2897	P	V$ETSF	CAAT_AP1F_01	CTGACCAATCAAGAG	-1046	P	V$CAAT
IRFF_ETSF_02	AGGGGAAGTTGAGATCCATCC	-2892	P	V$IRFF	CAAT_CAAT_01	GGAGCCAAACACTCT	-1020	P	V$CAAT
ETSF_ETSF_02	ACAAGCCAGGATGGATCTCAA	-2884	P	V$ETSF	P4		-978		
EGRF_NFAT_01	GCTGAGGAAATTATTTTAA	-2815	P	V$NFAT	NEUR_LHXF_02	ATGTCAACTGCTC	-965	P	V$NEUR
CEBP_CREB_01	CCCAGCTGAGGAAATTATTTT	-2812	P	V$CREB	NEUR_LHXF_02	TAAACGTGCAATTTAATAAGTCT	-899	P	V$LHXF
CEBP_CREB_01	CAGCTGAGGAAATTA	-2811	P	V$CEBP	STAT_IRFF_01	ACATAAAAATGAAACCTGCAC	-866	P	V$IRFF
HAND_GATA_02	ATTTCCTCAGCTGGGAGATTT	-2806	P	V$HAND	STAT_IRFF_01	TTATTTCCAAGAACACATA	-851	P	V$STAT
HAND_GATA_02	TATGGATATCCTA	-2789	P	V$GATA	STAT_FKHD_01	TGTGTTCTTGGAAATAAAC	-849	P	V$STAT
GATA_MYOD_01	GGGCCACAGTTGGCTGT	-2741	P	V$MYOD	STAT_FKHD_01	TGGAAATAAACAAAAAT	-842	P	V$FKHD
GATA_MYOD_01	GATCGATACCCGT	-2683	P	V$GATA	SORY_SORY_02	AATAAACAAAAATTGGTGTAATTCT	-834	P	V$SORY
SMAD_AP1F_03	CTGTGAGTCCAGA	-2651	P	V$AP1F	SORY_SORY_02	CACGAGAATTACACCAATTTTTGTT	-830	P	V$SORY
OCT1_CEBP_01	ACTATAGTAATTTGA	-2593	P	V$OCT1	PBXC_MYOD_01	TTCCTGGGTGACAGCTG	-783	P	V$PBXC
OCT1_CEBP_01	ATAGTTTTGAAAATT	-2583	P	V$CEBP	PBXC_MYOD_01	GGGTGACAGCTGCAATA	-778	P	V$MYOD
NFKB_SP1F_04	GATGTTTATTCCCTC	-2472	P	V$NFKB	SORY_ETSF_01	CATTGACAATATTGCAGCTGTCACC	-773	P	V$SORY
SMAD_EBOX_02	GAAGTCTGGAG	-2462	P	V$SMAD	P5		-765		
SMAD_AP1F_03	GAAGTCTGGAG	-2462	P	V$SMAD	IRFF_ETSF_01	TGGAGGAAGAGAAATCAGAGA	-738	P	V$IRFF
NFKB_SP1F_04	GCCCTGGGCAGAGGCCC	-2438	P	V$SP1F	ETSF_IRFF_01	TGGAGGAAGAGAAATCAGAGA	-738	P	V$IRFF
EGRF_SP1F_01	GATGTGGGCGGGACCAA	-2383	P	V$SP1F	SORY_ETSF_01	AGGATGGAGGAAGAGAAATCA	-734	P	V$ETSF
KLFS_SP1F_01	GATGTGGGCGGGACCAA	-2383	P	V$SP1F	IRFF_ETSF_01	AGGATGGAGGAAGAGAAATCA	-734	P	V$ETSF
KLFS_SP1F_01	AAGGTTGGGGCTGAAGG	-2367	P	V$KLFS	ETSF_IRFF_01	AGGATGGAGGAAGAGAAATCA	-734	P	V$ETSF
NR2F_SF1F_01	TTGCCAAGGACCCGT	-2278	P	V$SP1F	SP1F_YY1F_01	TTCCTCCATCCTAGACGCTGG	-725	P	V$YY1F
NR2F_SF1F_01	GGGTCCTTGGCAAAGAACACCTCCC	-2271	P	V$NR2F	SP1F_YY1F_01	GGCGGTGGCGGGGGTCG	-704	P	V$SP1F
NF1F_NR2F_01	TCCTTGGCAAAGAACACCTCC	-2270	P	V$NF1F	ETSF_SP1F_05	GGCGGTGGCGGGGGTCG	-704	P	V$SP1F
NF1F_NR2F_01	ATCATGGGGGCAAAGGGGAGGTGTT	-2256	P	V$NR2F	E2FF_SP1F_01	CGGTGGCGGGGGTCGGG	-702	P	V$E2FF
EBOX_SREB_01	AGATCATGGGGGCAA	-2249	P	V$SREB	ETSF_SP1F_05	GGGTCGGGGGAAGGGCTGGGC	-691	P	V$ETSF
EBOX_SREB_01	AAATCAGGAGATCAT	-2241	P	V$SREB	SP1F_ETSF_01	GGGTCGGGGGAAGGGCTGGGC	-691	P	V$ETSF
P2		-2170			E2FF_SP1F_01	GGGAAGGGCTGGGCCAG	-686	P	V$SP1F
CEBP_EBOX_01	TCTAATAAGTAAGGA	-1992	P	V$CEBP	SP1F_ETSF_01	GGGAAGGGCTGGGCCAG	-686	P	V$SP1F
SMAD_EBOX_02	TAGACACGTGCTC	-1982	P	V$EBOX	P6		-604		
CEBP_EBOX_01	TAGACACGTGCTC	-1982	P	V$EBOX	SP1F_MYOD_01	CGAGCGCAGGTGAGCAG	-542	P	V$MYOD
CREB_EBOX_02	GGTAGAGCACGTGTCTAATAA	-1982	P	V$CREB	CAAT_SREB_02	TGCTCACCTGCGCTC	-542	P	V$SREB
CREB_EBOX_02	TAGACACGTGCTC	-1982	P	V$EBOX	SP1F_ETSF_04	TGCAGTCCGGACTGCTCACCT	-533	P	V$ETSF
EBOX_SREB_01	TAGACACGTGCTC	-1982	P	V$EBOX	SP1F_ETSF_04	GCAGGGGGCGCCAATCT	-517	P	V$SP1F
EBOX_SREB_01	TAGACACGTGCTC	-1982	P	V$EBOX	SP1F_MYOD_01	GCAGGGGGCGCCAATCT	-517	P	V$SP1F
EBOX_SREB_01	AGAGCACGTGTCT	-1981	P	V$EBOX	CAAT_SREB_02	GGCGCCAATCTGCTT	-512	P	V$CAAT
EBOX_SREB_01	AGAGCACGTGTCT	-1981	P	V$EBOX	PBXC_MYOD_01	TGACAGCAGGTCGGGGC	-471	P	V$MYOD
EBOX_SREB_01	TCATCTCCAAATCAG	-1726	P	V$SREB	PBXC_MYOD_01	TGTCTGACTGACAGCAG	-463	P	V$PBXC
EBOX_SREB_01	AAATCAGGTTGCAGT	-1718	P	V$SREB	P7		-373		
SORY_SF1F_01	AACCCAAGGCTACAT	-1373	P	V$SF1F	NFAT_GATA_01	GCAAAGGAAAGTTCTTTCT	-202	P	V$NFAT

Table 4: Phosphorylation site on promoter model of mMC3r.

model NR2F_SF1F_01 at -2271 bp, from TF V$NR2F ; P site on model NF1F_NR2F_01 at -2270 bp, from TF V$NF1F ; P site on model NF1F_NR2F_01 at -2256 bp, from TF V$NR2F ; P site on model EBOX_SREB_01 at -2249 bp, from TF V$SREB ; P site on model EBOX_SREB_01 at -2241 bp, from TF V$SREB .

Between P2 and P3, there are P site on model CEBP_EBOX_01 at -1992 bp, from TF V$CEBP ; P site on model SMAD_EBOX_02 at -1982 bp, from TF V$EBOX ; P site on model CEBP_EBOX_01 at -1982 bp, from TF V$EBOX ; P site on model CREB_EBOX_02 at -1982 bp, from TF V$CREB ; P site on model CREB_EBOX_02 at -1982 bp, from TF V$EBOX ; P site on model EBOX_SREB_01 at -1982 bp, from TF V$EBOX ; P site on model EBOX_SREB_01 at -1982 bp, from TF V$EBOX ; P site on model EBOX_SREB_01 at -1981 bp, from TF V$EBOX ; P site on model EBOX_SREB_01 at -1981 bp, from TF V$EBOX ; P site on model EBOX_SREB_01 at -1726 bp, from TF V$SREB ; P site on model EBOX_SREB_01 at -1718 bp, from TF V$SREB ; P site on model SORY_SF1F_01 at -1373 bp, from TF V$SF1F ; P site on model SORY_SF1F_01 at -1317 bp, from TF V$SORY ; P site on model NF1F_NR2F_01 at -1250 bp, from TF V$NR2F ; P site on model NF1F_NR2F_01 at -1234 bp, from TF V$NF1F.

Between P3 and P4, there are P site on model CAAT_AP1F_01 at -1049 bp, from TF V$AP1F; P site on model CAAT_CAAT_01 at -1046 bp, from TF V$CAAT ; P site on model CAAT_AP1F_01 at -1046 bp, from TF V$CAAT ; P site on model CAAT_CAAT_01 at -1020 bp, from TF V$CAAT.

On P4 to P5, there are P site on model NEUR_LHXF_02 at -965 bp,

from TF V$NEUR ; P site on model NEUR_LHXF_02 at -899 bp, from TF V$LHXF ; P site on model STAT_IRFF_01 at -866 bp, from TF V$IRFF ; P site on model STAT_IRFF_01 at -851 bp, from TF V$STAT ; P site on model STAT_FKHD_01 at -849 bp, from TF V$STAT ; P site on model STAT_FKHD_01 at -842 bp, from TF V$FKHD ; P site on model SORY_SORY_02 at -834 bp, from TF V$SORY ; P site on model SORY_SORY_02 at -830 bp, from TF V$SORY ; P site on model PBXC_MYOD_01 at -783 bp, from TF V$PBXC ; P site on model PBXC_MYOD_01 at -778 bp, from TF V$MYOD ; P site on model SORY_ETSF_01 at -773 bp, from TF V$SORY.

On P5 to P6, there are P site on model IRFF_ETSF_01 at -738 bp, from TF V$IRFF ; P site on model ETSF_IRFF_01 at -738 bp, from TF V$IRFF ; P site on model SORY_ETSF_01 at -734 bp, from TF V$ETSF ; P site on model IRFF_ETSF_01 at -734 bp, from TF V$ETSF ; P site on model ETSF_IRFF_01 at -734 bp, from TF V$ETSF ; P site on model SP1F_YY1F_01 at -725 bp, from TF V$YY1F ; P site on model SP1F_YY1F_01 at -704 bp, from TF V$SP1F ; P site on model ETSF_SP1F_05 at -704 bp, from TF V$SP1F ; P site on model E2FF_SP1F_01 at -702 bp, from TF V$E2FF ; P site on model ETSF_SP1F_05 at -691 bp, from TF V$ETSF ; P site on model SP1F_ETSF_01 at -691 bp, from TF V$ETSF ; P site on model E2FF_SP1F_01 at -686 bp, from TF V$SP1F ; P site on model SP1F_ETSF_01 at -686 bp, from TF V$SP1F.

Between P6 and P7, there are P site on model SP1F_MYOD_01 at -542 bp, from TF V$MYOD ; P site on model CAAT_SREB_02 at -542 bp, from TF V$SREB ; P site on model SP1F_ETSF_04 at -533 bp, from TF V$ETSF ; P site on model SP1F_ETSF_04 at -517 bp, from TF V$SP1F ; P site on model SP1F_MYOD_01 at -517 bp, from TF V$SP1F ; P site on model CAAT_SREB_02 at -512 bp, from TF V$CAAT ; P site on model PBXC_MYOD_01 at -471 bp, from TF V$MYOD ; P site on model PBXC_MYOD_01 at -463 bp, from TF V$PBXC . On P7, there is P site on model NFAT_GATA_01 at -202 bp, from TF V$NFA.

Combine the DLA with the glycosylation-phosphorylation-site of mMC3r promoter model in one figure

After in silico data search, the glycosylation and phosphorylation site of promoter model on -3.2 kb of mMC3r 5'UTR (Figure 3) was plotted, then the DLA figure (Figure 1b) was plotted together with the glycosylation and phosphorylation site of mMC3r promoter model (Figure 3). As it shown in Figure 4a and 4b, the trend line of the DLA representing transcription activity, and the trend line of glycosylation relating to transcription regulation, was found to be negatively reciprocal. The corresponding trend line equation is shown (Figure 4c, Table 2) e.g., compare the DLA trend line (y=-8E-14x5 - 3E-10x4 - 4E-07x3 - 0.0003x2 - 0.071x - 4.1812) with the trend line of promoter model glycosylation (y=6E-13x5 + 2E-09x4 + 2E-06x3 + 0.0012x2 + 0.223x + 13.725), in the formula, each corresponding symbols are the opposite.

In addition, compare the trend lines of [P], [P]-[G] and [P]+[G] respectively with the trend line of DLA, it was shown, not only the glycosylation of the promoter model is negatively reciprocal related to the transcription activity, but also the phosphorylation, the combination of phosphorylation with glycosylation ([P]-[G], [P]+[G]) is in negatively reciprocal with the transcriptional activity. Since the glycosyaltion is nutritional and obesity related, the phosphorylation is signal sensing, it asks a question: either the nutritional or the signal components on the promoter model, will regulated the transcriptional activity in a negative reciprocal way?

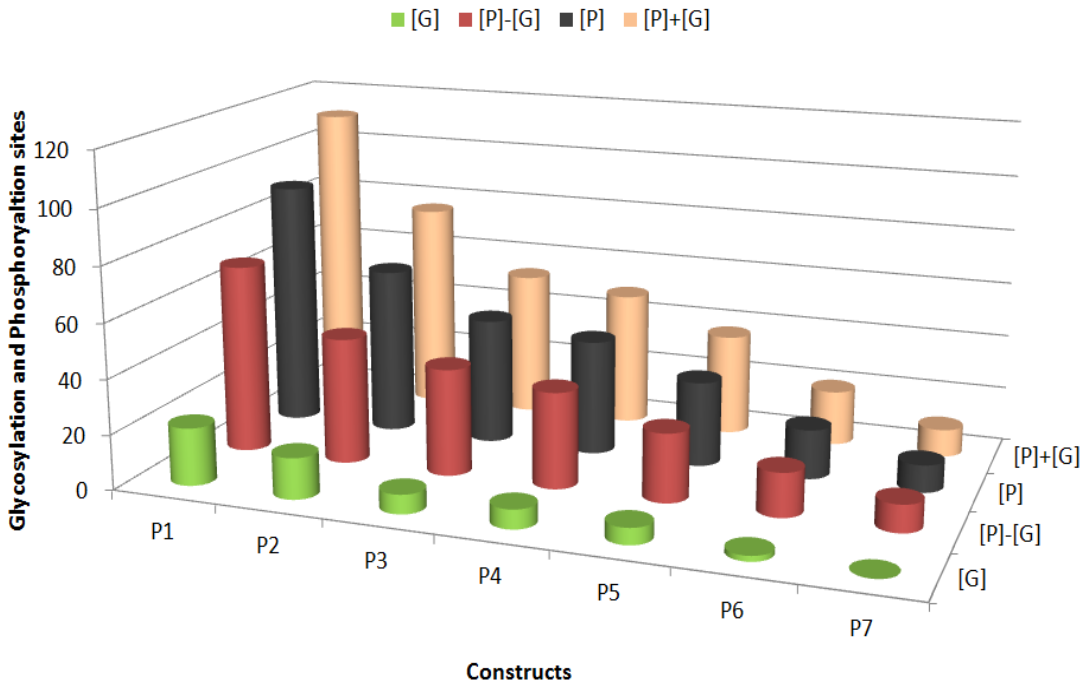

Figure 3: Glycosylation and phosphorylation sites of promoter models on mMC3r plasmid constructs P1-P7
[G]: number of glycosylation sites
[P]: number of phosphorylation sites
[P]-[G]: number difference between phosphorylation and glycosylation sites
[P]+[G]: sum of phosphorylation and glycosylation sites

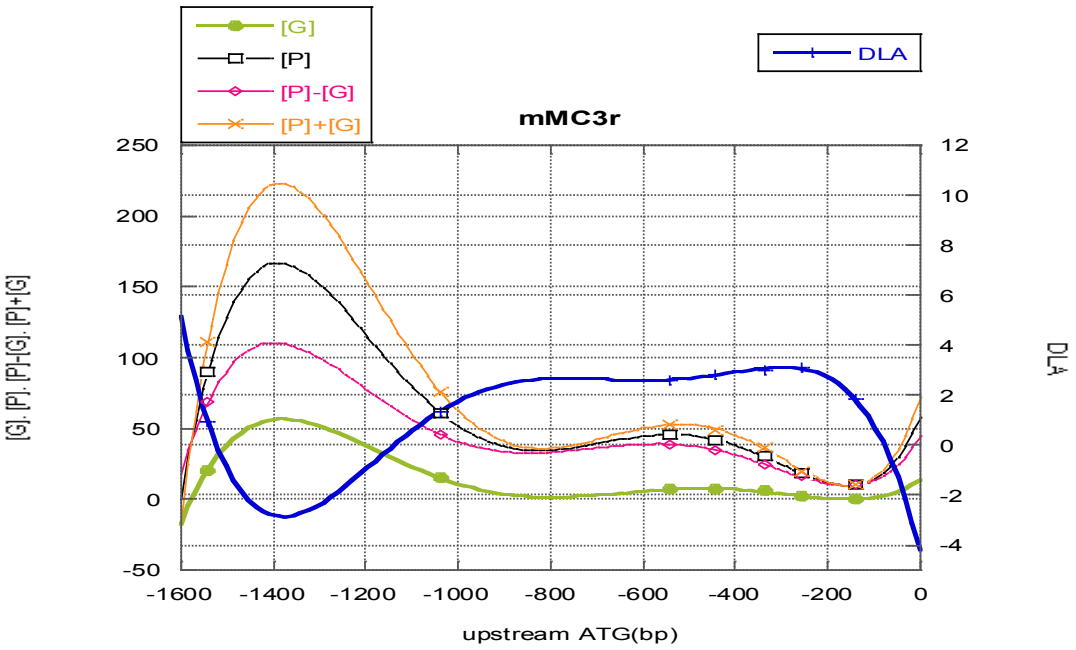

Figure 4a: combination plot of DLA with glycosylation and phosphorylation sites on promoter model of mMC3r.

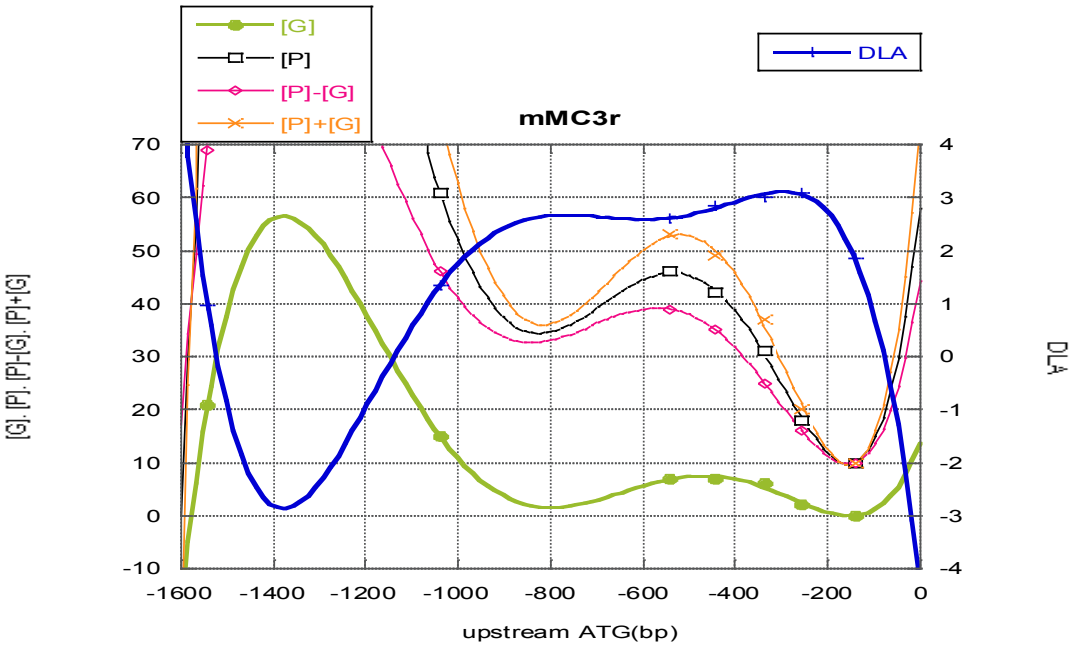

Figure 4b: combination plot of DLA with glycosylation and phosphorylation sites on promoter model of mMC3r (y axis expanded).

Acknowledgement

Thanks Dr. Herbert Geller for giving opportunity in a research environment. The author thanks her family members for their support.

References

1. Hunter T, Karin M (1992) The regulation of transcription by phosphorylation. Cell 70: 375-387.
2. Comer FI, Hart GW (1999) O-GlcNAc and the control of gene expression. Biochim Biophys Acta 1473: 161-171.
3. Myers MG Jr, Olson DP (2012) Central nervous system control of metabolism. Nature 491: 357-363.
4. Begriche K, Levasseur PR, Zhang J, Rossi J, Skorupa D, et al. (2011) Genetic dissection of the functions of the melanocortin-3 receptor, a seven-transmembrane G-protein-coupled receptor, suggests roles for central and peripheral receptors in energy homeostasis. J Biol Chem 286: 40771-40781.
5. Moro O, Ideta R, Ifuku O (1999) Characterization of the promoter region of the human melanocortin-1 receptor (MC1R) gene. Biochem Biophys Res Commun 262: 452-460.

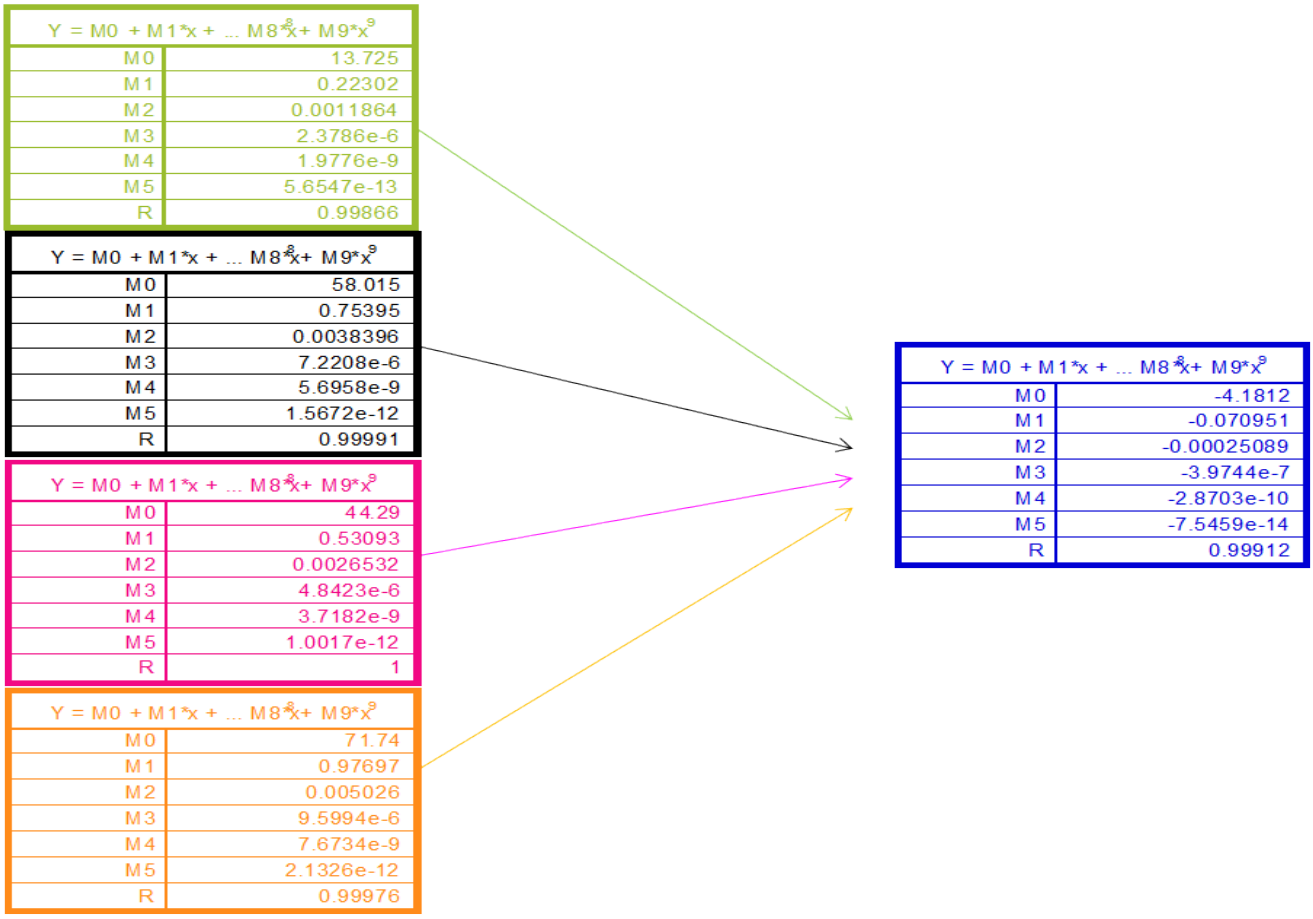

Figure 4c: Combination plot of DLA with glycosylation and phosphorylation sites on promoter model of mMC3r (with corresponding trend line equations and R square value).

6. Lubrano-Berthelier C, Cavazos M, Le Stunff C, Haas K, Shapiro A, et al. (2003) The human MC4R promoter: characterization and role in obesity. Diabetes 52: 2996-3000.

7. Sánchez E, Rubio VC, Cerdá-Reverter JM (2009) Characterization of the sea bass melanocortin 5 receptor: a putative role in hepatic lipid metabolism. J Exp Biol 212: 3901-3910.

8. Hanover JA, Krause MW, Love DC (2012) Bittersweet memories: linking metabolism to epigenetics through O-GlcNAcylation. Nat Rev Mol Cell Biol 13: 312-321.

9. Bohmann D (1990) Transcription factor phosphorylation: a link between signal transduction and the regulation of gene expression. Cancer Cells 2: 337-344.

10. Xin Wen, Wen Wei Zeng, Jack A Yanovski (2010) Determination of transcription starting site of Mus musculus Melanocortin 3 Receptor gene using “New 5’RACE”, Nature Protocol Exchange, doi:10.1038/nprot.2010.28.

11. Cartharius K, Frech K, Grote K, Klocke B, Haltmeier M, et al. (2005) MatInspector and beyond: promoter analysis based on transcription factor binding sites. Bioinformatics 21: 2933-2942.

12. X Wen, A Spitzer, Y Liu, DA Wailes, D Danley, et al. (2009) Determination of the transcriptional start sites of the mus musculus MC3r by 5’ RLM-RACE. 27th Annual Scientific Meeting of the Obesity Society.

13. Gonzalez GA, Montminy MR (1989) Cyclic AMP stimulates somatostatin gene transcription by phosphorylation of CREB at serine 133 Cell 59: 675-680.

14. Ying Liu, Anna Kamitakahara, Alice Joohee Kim, Greti Aguilera (2008) Cyclic Adenosine 3’,5’-Monophosphate Responsive Element Binding Protein Phosphorylation Is Required But Not Sufficient for Activation of Corticotropin-Releasing Hormone Transcription. Endocrinology 149: 3512-3520.